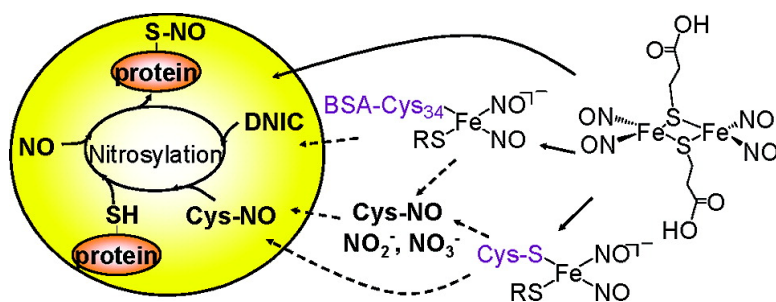


Nitric Oxide Physiological Responses and Delivery Mechanisms Probed by Water-Soluble Roussin's Red Ester and {Fe(NO)}⁺ DNIC

Yi-Ju Chen, Wei-Chi Ku, Li-Ting Feng, Ming-Li Tsai, Chung-Hung Hsieh, Wen-Hwei Hsu, Wen-Feng Liaw, Chen-Hsiung Hung, and Yu-Ju Chen

J. Am. Chem. Soc., **2008**, 130 (33), 10929-10938 • DOI: 10.1021/ja711494m • Publication Date (Web): 29 July 2008

Downloaded from <http://pubs.acs.org> on February 8, 2009



More About This Article

Additional resources and features associated with this article are available within the HTML version:

- Supporting Information
- Access to high resolution figures
- Links to articles and content related to this article
- Copyright permission to reproduce figures and/or text from this article

[View the Full Text HTML](#)

Nitric Oxide Physiological Responses and Delivery Mechanisms Probed by Water-Soluble Roussin's Red Ester and $\{\text{Fe}(\text{NO})_2\}^{10}$ DNIC

Yi-Ju Chen,^{†,‡} Wei-Chi Ku,^{‡,§,||} Li-Ting Feng,[‡] Ming-Li Tsai,[#] Chung-Hung Hsieh,[#] Wen-Hwei Hsu,[†] Wen-Feng Liaw,[#] Chen-Hsiung Hung,^{*,‡} and Yu-Ju Chen^{*,‡,||}

Institute of Molecular Biology, National Chung Hsing University, Taichung 402, Taiwan, Institute of Chemistry, Academia Sinica, Nankang, Taipei 115, Taiwan, Institute of Bioinformatics and Structural Biology, National Tsing Hua University, Hsinchu 30013, Taiwan, Chemical Biology and Molecular Biophysics, Taiwan International Graduate Program, Academia Sinica, Taipei 115, Taiwan, Department of Chemistry, National Changhua University of Education, Changhua, 50058 Taiwan, and Department of Chemistry, National Tsing Hua University, Hsinchu 30013, Taiwan

Received January 10, 2008; E-mail: yjchen@chem.sinica.edu.tw; chhung@chem.sinica.edu.tw

Abstract: Dinitrosyl-iron complexes (DNICs) are stable carriers for nitric oxide (NO), an important biological signaling molecule and regulator. However, the insolubility of synthetic DNICs, such as Roussin's red ester (RRE), in water has impaired efforts to unravel their biological functions. Here, we report a water-soluble and structurally well-characterized RRE $[\text{Fe}(\mu\text{-SC}_2\text{H}_4\text{COOH})(\text{NO})_2]_2$ (**DNIC-1**) and a $\{\text{Fe}(\text{NO})_2\}^{10}$ DNIC $[(\text{PPh}_2(\text{Ph-3-SO}_3\text{Na}))_2\text{Fe}(\text{NO})_2]$ (**DNIC-2**), their NO-induced protein regulation, and their cellular uptake mechanism using immortalized vascular endothelial cells as a model. Compared with the most common NO donor, S-nitroso-N-acetyl-penicillamine (SNAP), the *in vitro* NO release assay showed that both DNICs acted as much slower yet higher stoichiometric NO-release agents with low cytotoxicity ($\text{IC}_{50} > 1 \text{ mM}$). Furthermore, L-cysteine facilitated NO release from SNAP and **DNIC-1**, but not **DNIC-2**, in a dose- and time-dependent manner. EPR spectroscopic analysis showed, for the first time, that intact **DNIC-1** can either diffuse or be transported into cells independently and can transform to either paramagnetic protein bound DNIC in the presence of serum or $[\text{DNIC}(\text{Cys})_2]$ with excess L-cysteine under serum-free conditions. Both DNICs subsequently induced NO-dependent upregulation of cellular heat shock protein 70 and *in vivo* protein S-nitrosylation. We conclude that both novel water-soluble DNICs have potential to release physiologically relevant quantities of NO and can be a good model for deciphering how iron-sulfur-nitrosyl compounds permeate into the cell membrane and for elucidating their physiological significance.

Introduction

Nitric oxide (NO) produced by NO synthases is stabilized *in vivo*, presumably in the form of S-nitrosothiols (RSNOs)¹⁻⁴ and dinitrosyl iron complexes (DNICs),⁵⁻⁷ to preserve its physiological functionality in immune system regulation,⁸ smooth muscle relaxation,⁹ neurotransmission,¹⁰ cellular proliferation,^{11,12}

differentiation,¹³ and apoptosis.¹¹ DNICs have versatile biochemical functions, including upregulation of noradrenaline release in the rat tail artery, inhibition of glutathione reductase, and activation of the *Escherichia coli* SoxRS-Regulon by nitrosylation of enzymatically critical residues or $[\text{Fe-S}]$ clusters.¹⁴⁻¹⁶ Also, low-molecular-weight DNICs (LMW-DNIC) found in mammalian cells function as a physiologic regulator, especially in immune responses and cardiovascular systems.¹⁷

[†] National Chung Hsing University.

[‡] Institute of Chemistry, Academia Sinica.

[§] Institute of Bioinformatics and Structural Biology, National Tsing Hua University.

^{||} Taiwan International Graduate Program, Academia Sinica.

[‡] National Changhua University of Education.

[#] Department of Chemistry, National Tsing Hua University.

(1) Ignarro, L. J.; Lippton, H.; Edwards, J. C.; Baricos, W. H.; Hyman, A. L.; Kadowitz, P. J.; Gruetter, C. A. *J. Pharmacol. Exp. Ther.* **1981**, *218*, 739-749.

(2) Myers, P. R.; Minor, R. L.; Guerra, R.; Bates, J. N.; Harrison, D. G. *Nature* **1990**, *345*, 161-163.

(3) Girard, P.; Potier, P. *FEBS Lett.* **1993**, *320*, 7-8.

(4) Singh, R. J.; Hogg, J.; Joseph, J.; Kalyanaraman, B. *J. Biol. Chem.* **1996**, *271*, 18596-18603.

(5) Stone, J. R.; Marletta, M. A. *Biochemistry* **1994**, *33*, 5636-5640.

(6) Averill, B. A. *Chem. Rev.* **1996**, *96*, 2951-2964.

(7) Muller, B.; Kleschyov, A. L.; Alencar, J. L.; Vanin, A.; Stoclet, J.-C. *Ann. N.Y. Acad. Sci.* **2002**, *962*, 131-139.

(8) MacMicking, J.; Xie, Q.-w.; Nathan, C. *Annu. Rev. Immunol.* **1997**, *15*, 323-350.

(9) Ignarro, L.; Buga, G.; Wood, K.; Chaudhuri, G. *Proc. Natl. Acad. Sci. U.S.A.* **1987**, *84*, 9265-9269.

(10) Rand, M. J.; Li, C. G. *Annu. Rev. Physiol.* **1995**, *57*, 659-682.

(11) Carmeliet, P.; Dor, Y.; Herbert, J.-M.; Fukumura, D.; Brusselmans, K.; Dewerchin, M.; Neeman, M.; Bono, F.; Abramovitch, R.; Maxwell, P.; Koch, C. J.; Ratchliffe, P.; Moons, L.; Jain, R. K.; Collen, D.; Keshet, E. *Nature* **1998**, *394*, 485-490.

(12) Villalobo, A. *FEBS J.* **2006**, *273*, 2329-2344.

(13) Peunova, N.; Enikolopov, G. *Nature* **1995**, *375*, 68-73.

(14) Boese, M.; Keese, M. A.; Becker, K.; Busse, R.; Mulsch, A. *J. Biol. Chem.* **1997**, *272*, 21767-21773.

(15) Ding, H.; Dimple, B. *Proc. Natl. Acad. Sci. U.S.A.* **2000**, *97*, 5146-5150.

(16) Kleschyov, A.; Hubert, G.; Munzel, T.; Stoclet, J.-C.; Bucher, B. *BMC Pharmacol.* **2002**, *2*, 3.

For example, nitric oxide released from LMW-DNIC functions as an endothelium-derived relaxing factor to regulate hypotension and to induce relaxation of vascular smooth muscles by activating soluble guanylate cyclase.¹⁸ Moreover, injection of LMW-DNICs into rats caused the accumulation of heat shock protein 70 (HSP70) in the heart and blood.¹⁹ Furthermore, the {Fe(NO)₂} moiety of DNIC, when bound to glutathione transferases, were reported to serve as a signal to induce negative cooperativity.^{20–23}

In addition to monomeric LMW-DNICs, several synthetic iron–sulfur nitrosyls have been reported, including Roussin's black salt (RBS, [Fe₄S₃(NO)₇][−]),^{24,25} Roussin's red salt (RRS, [Fe₂S₂(NO)₄]^{2−}),²⁶ Roussin's red esters (RRE, Fe₂(SR)₂(NO)₄, R = aliphatic group),^{27–31} and cubane-like iron nitrosyl clusters such as tetranitrosyl-tetra-μ₃-sulfidotetrahydro-tetrairon ([Fe₄(NO)₄(μ₃-S)₄][−]).^{32,33} Among them the biological activities of RBS were extensively studied because of its lipophilicity and enhancement of NO release by photolysis.³⁴ RBS can effectively release NO in cell cultures as well as in vascular and brain tissues by photo/thermochemical delivery.^{35–37} In addition to vasodilator action, other biological activities of RBS were also explored, including inhibition of ADP-induced platelet aggregation³⁸ and lymphocyte proliferation,³⁹ bactericidal effects (see

reviews in ref 40), blockade of DNA synthesis,⁴¹ perturbation of cellular respiration,⁴² and induction of cell death in cancer cells.^{43,44} In contrast to RBS, RRE is usually insoluble in water, and therefore, scarce knowledge is known about the biological functions of RRE. To date, the only naturally occurring RRE is the carcinogenic [Fe₂(SMe)₂(NO)₄] discovered in pickled vegetables.^{45–47} However, it is not clear whether the cancer-causing effect of RRE is NO-dependent.

Transportation of RSNO across cell membrane through anion exchanger AE1,⁴⁸ cell-surface protein disulfide isomerase,^{49,50} and γ-glutamyl transpeptidase^{51,52} have been proposed. The unstable S-nitrosocysteine (CysNO) derived from trans-nitrosylation between S-nitrosoglutathione/S-nitroso-N-acetylpenicillamine (SNAP) and L-cysteine^{53–56} is transported across the cell membrane by the amino acid transporter system L (LAT).^{55,57,58} Exogenously administered LMW-DNICs were reported to transport via circulating blood to the liver and kidney and permeate these tissues through an unidentified intermediate.⁵⁸ A very recent study reported that *in situ* generation of stable LMW-DNICs induced hypotension in conscious normotensive and hypertensive rats, suggesting the potential action of LMW-DNICs as hypotensive drugs.⁵⁹ It was hypothesized that formation of NO radicals and protein-bound DNICs were responsible for the observed hypotension.⁵⁹ Administration of RBS into the lumen of isolated rat artery resulted in the retention of RBS within the intimal layers of the artery walls, suggesting RBS can penetrate through the endothelial cell membrane.³⁶ For RRE, however, it remains to be investigated whether RRE can directly diffuse into cells or be transported into cells through

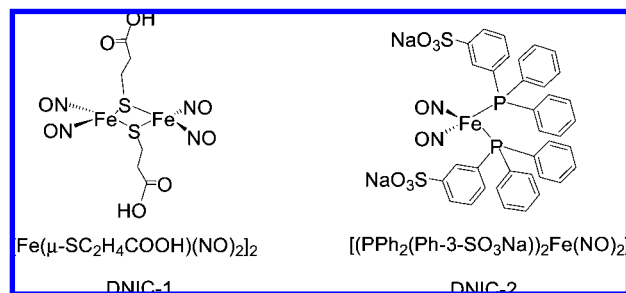
- (17) Ueno, T.; Yoshimura, T. *Jpn. J. Pharmacol* **2000**, *82*, 95–101.
- (18) Mulsch, A.; Mordvintsev, P.; Vanin, A. F.; Busse, R. *FEBS Lett.* **1991**, *294*, 252–256.
- (19) Malyshev, I. Y.; Malugin, A. V.; Golubeva, L. Y.; Zenina, T. A.; Manukhina, E. B.; Mikoyan, V. D.; Vanin, A. F. *FEBS Lett.* **1996**, *391*, 21–23.
- (20) Bello, M. L.; Nuccetelli, M.; Caccuri, A. M.; Stella, L.; Parker, M. W.; Rossjohn, J.; McKinstry, W. J.; Mozzi, A. F.; Federici, G.; Polizio, F.; Pedersen, J. Z.; Ricci, G. *J. Biol. Chem.* **2001**, *276*, 42138–42145.
- (21) Cesareo, E.; Parker, L. J.; Pedersen, J. Z.; Nuccetelli, M.; Mazzetti, A. P.; Pastore, A.; Federici, G.; Caccuri, A. M.; Ricci, G.; Adams, J. J.; Parker, M. W.; Bello, M. L. *J. Biol. Chem.* **2005**, *280*, 42172–42180.
- (22) Maria, F. D.; Pedersen, J. Z.; Caccuri, A. M.; Antonini, G.; Turella, P.; Stella, L.; Bello, M. L.; Federici, G.; Ricci, G. *J. Biol. Chem.* **2003**, *278*, 42283–42293.
- (23) Turella, P.; Pedersen, J. Z.; Caccuri, A. M.; De Maria, F.; Mastroberardino, P.; Bello, M. L.; Federici, G.; Ricci, G. *J. Biol. Chem.* **2003**, *278*, 42294–42299.
- (24) Roussin, F. Z. *Ann. Chim. Phys.* **1858**, *52*, 285.
- (25) Brauer, G. *Handbook of preparative inorganic chemistry*; Academic Press: New York, 1963.
- (26) Seyferth, D.; Gallagher, M. K. *Organometallics* **1986**, *5*, 539–548.
- (27) Bladon, P.; Dekker, M.; Knox, G. R.; Willison, D.; Jaffari, G. A. *Organometallics* **1993**, *12*, 1725–1741.
- (28) Butler, A. R.; Glidewell, C.; Hyde, A. R.; Walton, J. C. *Polyhedron* **1985**, *4*, 797–809.
- (29) Butler, A. R.; Glidewell, C.; Glidewell, S. M. *J. Chem. Soc., Chem. Commun.* **1992**, 141–142.
- (30) Weckslers, S. R.; Hutchinson, J.; Ford, P. C. *Inorg. Chem.* **2006**, *45*, 1192–1200.
- (31) Weckslers, S. R.; Mikhailovsky, A.; Korystov, D.; Buller, F.; Kannan, R.; Tan, L. S.; Ford, P. C. *Inorg. Chem.* **2007**, *46*, 395–402.
- (32) Gall, R. S.; Chu, C. T. W.; Dahl, L. F. *J. Am. Chem. Soc.* **1974**, *96*, 4019–4023.
- (33) Chu, T.-W. C.; Lo, Y.-K. F.; Dahl, L. F. *J. Am. Chem. Soc.* **1982**, *104*, 3409–3422.
- (34) Butler, A. R.; Megson, I. L. *Chem. Rev.* **2002**, *102*, 1155–1166.
- (35) Butler, A. R.; Flitney, F. W.; Rhodes, P. *Pers. Bioinorg. Chem.* **1996**, *3*, 251–277.
- (36) Flitney, F. W.; Megson, I. L.; Flitney, D. E.; Butler, A. R. *Br. J. Pharmacol.* **1992**, *107*, 842–848.
- (37) Flitney, F. W.; Megson, I. L.; Thomson, J. L.; Kennovin, G. D.; Butler, A. R. *Br. J. Pharmacol.* **1996**, *117*, 1549–1557.
- (38) Ludbrook, S. B.; Scrutton, M. C.; Joannou, C. L.; Cammack, R.; Hughes, M. N. *Platelets* **1995**, *6*, 209–212.
- (39) Rowland, I. J.; Denham, S.; Butler, A. R.; Flitney, D. E.; Megson, I. L. In *Biology of Nitric Oxide*; Moncada, S.; Marletta, M. A.; Hibbs, J. B., Higgs, E. A., Eds.; Portland Press: London, 1992; Vol. 2.
- (40) Cammack, R.; Joannou, C. L.; Cui, X. Y.; Torres Martinez, C.; Maraj, S. R.; Hughes, M. N. *Biochim. Biophys. Acta* **1999**, *1411*, 475–488.
- (42) Hurst, R. D.; Chowdhury, R.; Clark, J. B. *J. Neurochem.* **1996**, *67*, 1200–1207.
- (41) Delaney, C. A.; Green, I. C.; Lowe, J. E.; Cunningham, J. M.; Butler, A. R.; Renton, L.; D'Costa, I.; Green, M. H. *Mutat. Res.* **1997**, *375*, 137–146.
- (43) Janczyk, A.; Wolnicka-Glubisz, A.; Chmura, A.; Elas, M.; Matuszak, Z.; Stochel, G.; Urbanska, K. *Nitric Oxide* **2004**, *10*, 42–50.
- (44) Bourassa, J.; DeGraff, W.; Kudo, S.; Wink, D. A.; Mitchell, J. B.; Ford, P. C. *J. Am. Chem. Soc.* **1997**, *119*, 2853–2860.
- (45) Liu, J.-G.; Li, M.-H. *Carcinogenesis* **1989**, *10*, 617–620.
- (46) Zhang, W. X.; Xu, M. S.; Wang, G. H.; Wang, M. Y. *Cancer Res.* **1983**, *43*, 339–341.
- (47) Zhu, P.; Sang, Y.; Xu, H.; Zhao, J.; Xu, R.; Sun, Y.; Xu, T.; Wang, X.; Chen, L.; Feng, H.; Li, C.; Zhao, S. *Biochem. Biophys. Res. Commun.* **2005**, *331*, 938–946.
- (48) Pawloski, J. R.; Hess, D. T.; Stamler, J. S. *Nature* **2001**, *409*, 622–626.
- (49) Ramachandran, N.; Root, P.; Jiang, X.-M.; Hogg, P. J.; Mutus, B. *Proc. Natl. Acad. Sci. U.S.A.* **2001**, *98*, 9539–9544.
- (50) Yaroslavskiy, B. B.; Zhang, Y.; Kalla, S. E.; Palacios, V. G.; Sharrow, A. C.; Li, Y.; Zaidi, M.; Wu, C.; Blair, H. C. *J. Cell Sci.* **2005**, *118*, 5479–5487.
- (51) Groote, M. A. D.; Granger, D.; Xu, Y.; Campbell, G.; Prince, R.; Fang, F. C. *Proc. Natl. Acad. Sci. U.S.A.* **1995**, *92*, 6399–6403.
- (52) Hogg, N.; Singh, R. J.; Konorev, E.; Joseph, J.; Kalyanaraman, B. *Biochem. J.* **1997**, *323*, 477–481.
- (53) Satoh, S.; Kimura, T.; Toda, M.; Miyazaki, H.; Ono, S.; Narita, H.; Murayama, T.; Nomura, Y. *J. Cell. Physiol.* **1996**, *169*, 87–96.
- (54) Satoh, S.; Kimura, T.; Toda, M.; Maekawa, M.; Ono, S.; Narita, H.; Miyazaki, H.; Murayama, T.; Nomura, Y. *J. Neurochem.* **1997**, *69*, 2197–2205.
- (55) Padgett, C. M.; Whorton, A. R. *Am. J. Physiol. Cell Physiol.* **1997**, *272*, C99–108.
- (56) Mallis, R. J.; Thomas, J. A. *Arch. Biochem. Biophys.* **2000**, *383*, 60–69.
- (57) Zhang, Y.; Hogg, N. *Proc. Natl. Acad. Sci. U.S.A.* **2004**, *101*, 7891–7896.
- (58) Li, S.; Whorton, A. R. *J. Biol. Chem.* **2005**, *280*, 20102–20110.
- (59) Lakomkin, V. L.; Vanin, A. F.; Timoshin, A. A.; Kapelko, V. I.; Chazov, E. I. *Nitric Oxide* **2007**, *16*, 413–418.
- (60) Graziano, M.; Lamattina, L. *Trends Plant Sci.* **2005**, *10*, 4–8.

unidentified transporters⁶⁰ in the forms of protein-bound DNICs or LMW-DNICs.

In the earlier biomimetic model study, we and others have shown that the most straightforward and facile pathway for the formation of the anionic $\{Fe(NO)_2\}^9$ DNICs $[(RS)_2Fe(NO)_2]^-$ is the direct nitrosylation of $[Fe_m(SR)_n]^{x-}$ clusters (e.g., $[Fe(SR)_4]^{2-/-1-}$ and $[(RS)_2Fe(\mu-S)_2Fe(SR)_2]^{2-}$).^{61–63} Presumably, the formation of DNICs through the combination of Fe^{2+} , RSH, and NO may occur through the formation of $[Fe_m(SR)_n]^{x-}$ clusters followed by nitrosylation. In particular, the interconversion among the anionic/neutral $\{Fe(NO)_2\}^9$ DNICs, $\{Fe(NO)_2\}^{10}$ DNICs, and RRE has been hypothesized to occur in biological systems.^{61,64–68} Extensive EPR spectroscopic studies have identified nitrosyl nonheme iron complexes as products of the interaction of NO with several iron–sulfur and other iron-containing proteins.^{34,69–78} EPR spectroscopy has also been used to monitor the formation of DNICs during the conversion of active aconitase containing a $[3Fe-4S]$ cluster to its apo-form triggered by NO.⁷⁰ In comparison with paramagnetic DNICs, the physiological roles of RRE are hard to define due to the lack of EPR signal resulting from the antiferromagnetic coupling between the two $\{Fe(NO)_2\}^9$ cores. The exploration of RRE-related biological functions is also limited because of difficulty in obtaining water-soluble, crystallographically pure RRE. To discover the possible RRE-mediated biological implementations through direct permeate or unknown interconversion among RRE, LMW-DNICs, or protein-bound DNICs, it is important to study the transformation of different DNIC forms through spectroscopic methods such as EPR on a water-soluble RRE with well-defined structural characterization.

As opposed to previously *in situ* generated DNIC species, herein we synthesized a water-soluble, structurally well-characterized RRE, $[Fe(\mu-SC_2H_4COOH)(NO)_2]_2$ (**DNIC-1**), and a $\{Fe(NO)_2\}^{10}$ DNIC, $[(PPh_2(Ph-3-SO_3Na))_2Fe(NO)_2]$ (**DNIC-2**), as shown in Scheme 1. In addition to evaluation of cytotoxicity on the model immortalized vascular endothelial cell line,

Scheme 1



EA.hy926, we demonstrated a slow yet differential level of NO release from **DNIC-1** and **DNIC-2**. The subsequent cellular responses and potential biological implementations of DNICs in vascular endothelial cells were studied by induction of protein S-nitrosylation and NO-dependent accumulation of HSP70. Finally, we propose a possible mechanism for structural conversion of **DNIC-1** in aqueous solution and its permeation into the cell membrane based on EPR spectroscopic evidence.

Experimental Section

Reagents and Chemicals. Unless specified, all reagents and chemicals used in this study were purchased from Sigma.

Manipulations, reactions, and transfers were conducted under nitrogen, according to Schlenk techniques or in a glovebox (argon gas). Solvents were distilled under nitrogen using appropriate drying agents (diethyl ether from CaH_2 ; acetonitrile from $CaH_2-P_2O_5$; methylene chloride from CaH_2 ; hexane and tetrahydrofuran (THF) from sodium benzophenone) and were stored in dried, N_2 -filled flasks over 4-Å molecular sieves. These solvents were purged with N_2 before use. Solvents were transferred to reaction vessels via stainless cannula under positive N_2 pressure. The iron pentacarbonyl, sodium nitrite, 3-mercaptopropionic acid, and diphenylphosphinobenzene-3-sulfonic acid sodium salt were used as received. The compound $Fe(CO)_2(NO)_2$ was synthesized according to published procedures.^{79–81} Infrared spectra of the $\nu(NO)$ and $\nu(COO)$ stretching frequencies were recorded on a PerkinElmer model spectrum one B spectrophotometer with sealed solution cells (0.1 mm, KBr windows) or KBr solid. UV–vis spectra were recorded on a GBC Cintra 10e and Jasco V-570. Analyses of carbon, hydrogen, and nitrogen were obtained with a CHN analyzer (Heraeus).

Preparation of $[Fe(\mu-SC_2H_4COOH)(NO)_2]_2$ (DNIC-1**).** The compound 3-mercaptopropionic acid (90 μ L, 1 mmol) was dissolved in THF (4 mL) in a 25-mL Schlenk flask, and a THF solution (5 mL) of $Fe(CO)_2(NO)_2$ (1 mmol) was prepared freshly and was added to the flask by cannula under positive N_2 pressure at 0 °C. The resulting solution was stirred at ambient temperature overnight. Solvent was then removed under vacuum. The yellow-brown crude solid was redissolved in THF and then filtered through Celite. Addition of hexane to the yellow-brown filtrate led to the precipitation of yellow-brown solid $[Fe(\mu-SC_2H_4COOH)(NO)_2]_2$ (**DNIC-1**) (yield 0.132 g, 60%). X-ray-quality crystals were obtained by diffusion of hexane (1:1 volume ratio) into the THF solution of complex **DNIC-1** at -20 °C for 3 weeks. IR_{NO}: 1751 s, 1772 s, 1811 vw (THF) cm^{-1} . The absorption spectrum of THF was as follows [λ_{max} , nm (ϵ , $M^{-1} cm^{-1}$): 362 (9116), 425 (4540), 755 (109)]. Calcd for $C_6H_{10}Fe_2N_4O_8S_2$: C, 16.3; H, 2.28; N, 12.68. Found: C, 17.16; H, 2.92; N, 12.31.

(79) Hedberg, L. H., K.; Satija, S. K.; Swanson, B. I. *Inorg. Chem.* **1985**, *24*, 2766–2771.

(80) Teo, B. K.; Hall, M. B.; Fenske, R. F.; Dahl, L. F. *J. Organomet. Chem.* **1974**, *70*, 413–420.

(81) Crayston, J. A.; Glidewell, C.; Lambert, R. J. *Polyhedron* **1990**, *9*, 1741–1746.

- (61) Lu, T. T.; Chiou, S. J.; Chen, C. Y.; Liaw, W. F. *Inorg. Chem.* **2006**, *45*, 8799–8806.
- (62) Harrop, T. C.; Song, D.; Lippard, S. J. *J. Am. Chem. Soc.* **2006**, *128*, 3528–3529.
- (63) Harrop, T. C.; Song, D.; Lippard, S. J. *J. Inorg. Biochem.* **2007**, *101*, 1730–1738.
- (64) Tsai, M. L.; Liaw, W. F. *Inorg. Chem.* **2006**, *45*, 6583–6585.
- (65) Tsai, M. L.; Chen, C. C.; Hsu, I. J.; Ke, S. C.; Hsieh, C. H.; Chiang, K. A.; Lee, G. H.; Wang, Y.; Chen, J. M.; Lee, J. F.; Liaw, W. F. *Inorg. Chem.* **2004**, *43*, 5159–5167.
- (66) Tsai, F. T.; Chiou, S. J.; Tsai, M. C.; Tsai, M. L.; Huang, H. W.; Chiang, M. H.; Liaw, W. F. *Inorg. Chem.* **2005**, *44*, 5872–5881.
- (67) Hung, M. C.; Tsai, M. C.; Lee, G. H.; Liaw, W. F. *Inorg. Chem.* **2006**, *45*, 6041–6047.
- (68) Chen, T.-N.; Lo, F.-C.; Tsai, M.-L.; Shih, K.-N.; Chiang, M.-H.; Lee, G.-H.; Liaw, W.-F. *Inorg. Chim. Acta* **2006**, *359*, 2525–2533.
- (69) Drapier, J. C.; Pellat, C.; Henry, Y. *J. Biol. Chem.* **1991**, *266*, 10162–10167.
- (70) Kennedy, M. C.; Antholine, W. E.; Beinert, H. *J. Biol. Chem.* **1997**, *272*, 20340–20347.
- (71) Lepoivre, M.; Flaman, J. M.; Bobe, P.; Lemaire, G.; Henry, Y. *J. Biol. Chem.* **1994**, *269*, 21891–21897.
- (72) Morse, R. H.; Chan, S. I. *J. Biol. Chem.* **1980**, *255*, 7876–7882.
- (73) Lee, M.; Arosio, P.; Cozzi, A.; Chasteen, N. D. *Biochemistry* **1994**, *33*, 3679–3687.
- (74) Sellers, V. M.; Johnson, M. K.; Dailey, H. A. *Biochemistry* **1996**, *35*, 2699–2704.
- (75) Foster, M. W.; Cowan, J. A. *J. Am. Chem. Soc.* **1999**, *121*, 4093–4100.
- (76) Vanin, A. F.; Malenkova, I. V.; Serezhenkov, V. A. *Nitric Oxide* **1997**, *1*, 191–203.
- (77) Ford, P. C.; Bourassa, J.; Miranda, K.; Lee, B.; Lorkovic, I.; Boggs, S.; Kudo, S.; Laverman, L. *Coord. Chem. Rev.* **1998**, *171*, 185–202.
- (78) Vanin, A. F. *Biochemistry (Moscow, Russ. Fed.)* **1998**, *63*, 782–793.

Preparation of [(PPh₂(Ph-3-SO₃Na))₂Fe(NO)₂] (PPh₂(Ph-3-SO₃Na) = Diphenylphosphinobenzene-3-sulfonic Acid Sodium Salt) (DNIC-2). A THF solution of complex [Fe(μ -SC₆H₄-o-NHC(O)Ph)(NO)₂]₂ (0.2 mmol), prepared freshly from the reaction of Fe(CO)₂(NO)₂ (0.4 mmol) and bis(*o*-benzamidophenyl) disulfide (0.2 mmol, 0.091 g) in THF (5 mL), was transferred to a 50-mL Schlenk flask loaded with diphenylphosphinobenzene-3-sulfonic acid sodium salt (0.144 g, 0.4 mmol) by a cannula under positive N₂ pressure at ambient temperature. The reaction was stirred for 1 h. The solution was then concentrated, and diethyl ether was added to precipitate a dark brown solid. The resulting mixture was then filtered to separate the brown solid [(PPh₂(Ph-3-SO₃Na))₂Fe(NO)₂] (DNIC-2) (yield 0.298 g, 88%). IR (ν_{NO}): 1672, 1715 cm⁻¹ (THF). Absorption spectrum (THF) [λ_{max} , nm (ϵ , M⁻¹ cm⁻¹): 424 (320), 538 (71). HR-FAB MS m/z 844.9974 [M + H]⁺ (calcd for C₃₆H₂₉O₈N₂P₂S₂Na₂Fe, 844.9985); FAB-MS m/z 844.1 [M + H]⁺.

Cell Line and Cell Culture Conditions. EA.hy926 cells were kindly provided by Dr. Tzu-Ching Meng (Institute of Biological Chemistry, Academia Sinica, Taipei, Taiwan). The cell line originated from the fusion of primary human umbilical vein endothelial cells with a human lung carcinoma and has been used as a model for studying the physiological changes of endothelial cells in response to environmental stimuli.⁸² Cells were cultured at 37 °C, 5% CO₂ in Dulbecco's Modified Eagle's Medium with low glucose (1000 mg/L) (HyClone), supplemented with 10% heat-inactivated fetal bovine serum (GibcoBRL) and Antibiotic-Antimycotic (GibcoBRL), which contained 100 U/mL penicillin, 100 μ g/mL streptomycin, and 0.25 μ g/mL amphotericin B.

Determination of Cytotoxicity by MTT Assay. The potential cytotoxicity of NO donors containing SNAP (Calbiochem), water-soluble DNIC-1, and DNIC-2 was determined by a quantitative colorimetric method using a 3-(4,5-dimethyl-2-thiazolyl)-2,5-diphenyl-2H-tetrazolium bromide (MTT) assay⁸³ with minor modifications. Briefly, EA.hy926 cells were inoculated at a density of 5000 cells per well in 96-well cell culture plates and incubated for 12 h. Different concentrations of NO donors dissolved in fresh complete medium were added to the cell culture and further incubated for 24 h. The medium was removed, 100 μ L per well of 0.1 mg/mL MTT in fresh medium were added to each well, and cultured at 37 °C, 5% CO₂ for 4 h. After the medium was removed, the formazan crystals formed in the cells were dissolved in 100 μ L of dimethyl sulfoxide (Pierce). The absorbance was measured at 570 nm using a SpectraMax M5 Microplate Reader (Molecular Devices). All experiments were performed in triplicate.

Quantitative Analysis of NO Release by Total Nitrite Assay. The temporal release of NO by NO donors into the culture medium was quantified using a total nitrite assay kit (R&D systems) following the manufacturer's instructions. In brief, 1.0 \times 10⁵ cells per well were inoculated in 12-well cell culture plates for 12 h. Various concentrations of NO donors with or without equal molar L-cysteine were added into the cell culture and further incubated for 30 min, 2 h, 6 h, or 24 h. At each time point, culture medium was collected, diluted 5-fold using Reaction Diluent provided in the kit, and transferred to a new 96-well cell culture plate. In parallel, a serial dilution of nitrate standard solutions provided in the kit was also prepared. NADH and diluted (5-fold) nitrate reductase were added to each well and were incubated at 37 °C for 30 min. Griess Reagents I and II were added to each well, mixed by tapping the side of the plate gently, and the plate was incubated at room temperature for 10 min. The absorbance was determined at 540 nm with a wavelength correction at 690 nm using a SpectraMax M5 Microplate Reader. Total nitrites released by NO donors were quantified with reference to the nitrate standard curve. For cell-free experiments, NO donors were directly added to fresh medium for 30 min, 2 h, 6 h, or 24 h, and the released nitrites

were determined as described above. In all experiments, each condition was performed in triplicate.

Detection of Paramagnetic Intermediates from DNIC-1 by Electron Paramagnetic Resonance (EPR) Spectroscopy. Cells were inoculated at 3.5 \times 10⁶ cells per dish in 15-cm cell culture dishes and incubated at 37 °C for 12 h. DNIC-1 was added to the cell cultures at final concentration of 300 μ M for 15 min or 6 h. If needed, an equal concentration of L-cysteine was also added to the cell culture. SNAP/L-cysteine (1.2 mM) with or without 25 mM iron(II) sulfate was added into the control medium or cultured cells for 15 min. At each time point, the culture medium was collected, passed through a 0.22- μ m filter (Millipore) to remove particles, and frozen in liquid nitrogen. In parallel, cultured cells on the dish were washed three times with ice-cold phosphate-buffered saline, scraped, centrifuged at 1000 \times g for 1 min, resuspended with 200 μ L of phosphate-buffered saline, and frozen in liquid nitrogen. For each EPR measurement, 1.5 \times 10⁷ cells were used. Samples were transferred to EPR tubes (Wilmad LabGlass) and subjected to EPR analysis using a Bruker E580 pulse and CW spectrometer (Bruker). All spectra were recorded at -196 °C with a microwave power of 1 mW, modulation frequency of 100 kHz, modulation amplitude of 5 G, time constant of 163.84 ms, and conversion time of 20.48 ms. For control medium experiments, 10% fetal bovine serum, 1% bovine serum albumin (BSA), various concentrations of L-cysteine (0.3 to 6 mM), or ethylenediaminetetraacetic acid (EDTA, 0 to 5 mM) were added into fresh media and incubated for 15 min. At each time point, medium was collected and subjected to EPR analysis as described above.

Measurement of HSP70 Induction by Western Blotting. Cells were treated with different NO donors, harvested, and washed three times with ice-cold phosphate-buffered saline. Total lysate was prepared by resuspending the cells in SDS-PAGE sample buffer (60 mM Tris-HCl, pH 6.8, 10% (v/v) glycerol, 2% (w/v) SDS, 0.005% (w/v) bromophenol blue, and 0.7 M β -mercaptoethanol), sonicated using Bioruptor (Cosmo Bio, Tokyo, Japan), and heated at 95 °C for 5 min. Protein concentration was determined with the bicinchoninic acid (BCA) assay reagent (Pierce). Total lysate (1 μ g) was separated by 10% SDS-PAGE. Heat-shocked HeLa cell total lysates (2 μ g; StressGen Biotechnologies) were loaded in parallel to serve as positive controls. Protein bands were then electrophoretically transferred to a polyvinylidene fluoride (PVDF) membrane (Millipore), and the membrane was incubated in blocking buffer containing 5% nonfat milk in TTBS (20 mM Tris-HCl, pH 7.4, 137 mM NaCl, 2.6 mM KCl, and 0.05% (v/v) Tween-20) at room temperature for 1 h. The membrane was incubated with mouse monoclonal anti-HSP70 (StressGen Biotechnologies) at a 1:10 000 dilution in blocking buffer at room temperature for 1 h followed by washing four times in TTBS at room temperature for 5 min. The membrane was then incubated with goat anti-mouse IgG conjugated with horseradish peroxidase (Santa Cruz Biotechnology) at 1:5000 dilution in blocking buffer. After the membrane was washed four times in TTBS at room temperature for 5 min, the immunopositive bands on the membrane were visualized using the enhanced chemiluminescence (ECL) detection system (Millipore).

Detection of Protein S-Nitrosylation by the Biotin Switch Method. Detection of protein S-nitrosylation was performed by the biotin switch method⁸⁴ with modifications. Cells were treated with 300 μ M DNIC-1 with equal molar L-cysteine at 37 °C for 30 min, 1 h, 2 h, 6 h, or 24 h in the dark. At each time point, total lysate was prepared by resuspending cells in lysis buffer, which contained HEN buffer (250 mM HEPES, pH 7.7, 1 mM EDTA, and 0.1 mM neocuproine), 1% Nonidet P-40, 150 mM NaCl, 1 mM PMSF, and 20 mM iodoacetamide. Cellular debris was removed by centrifugation at 16 000 \times g at 4 °C for 15 min. Protein concentration was determined by the BCA assay (Pierce). To block free cysteines on proteins, three volumes of blocking buffer (270 mM of iodoaceta-

(82) Edgell, C. J.; McDonald, C. C.; Graham, J. B. *Proc. Natl. Acad. Sci. U.S.A.* **1983**, *80*, 3734–3737.

(83) Mosmann, T. J. *Immunol. Meth.* **1983**, *65*, 55–63.

(84) Jaffrey, S. R.; Erdjument-Bromage, H.; Ferris, C. D.; Tempst, P.; Snyder, S. H. *Nat. Cell Biol.* **2001**, *3*, 193–197.

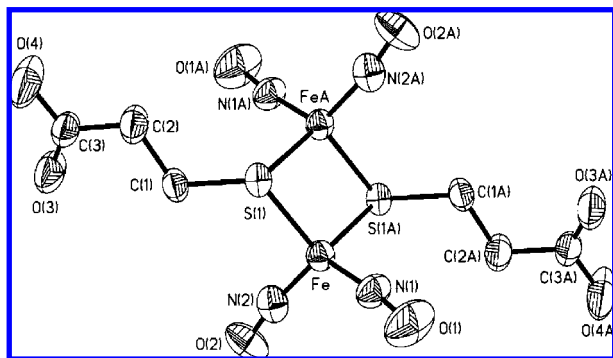


Figure 1. Crystal structure and labeling scheme of **DNIC-1** with thermal ellipsoids drawn at 50% probability. Selected bond distances (Å) and angles (deg): Fe–N(1), 1.672(8); Fe–N(2), 1.688(10); Fe–S(1), 2.264(3); Fe···Fe(A), 2.710(3); N(1)–O(1), 1.143(12); N(2)–O(2), 1.141(12); N(2)–Fe–N(1), 118.8(4); N(1)–Fe–S(1), 106.9(3); N(2)–Fe–S(1), 110.2(3); O(1)–N(1)–Fe, 171.5(10); O(2)–N(2)–Fe, 171.0(9).

mid in HEN buffer containing 5% (w/v) SDS) were added to the total lysate and incubated at 50 °C for 30 min in the dark with shaking at 50 rpm. After blocking, 10 volumes of –20 °C ice-cold acetone were added and the entire solution was incubated at –20 °C for 1.5 h to precipitate proteins. The protein pellet was recovered by centrifugation at 10 000 × g for 15 min and washed three times with 95% cold ethanol. Each pellet was resuspended in HEN buffer containing 1% SDS, and the protein concentration was determined by BCA assay. Free sulfhydryl groups in proteins were reduced in a buffer containing a 1/50 volume of 250 mM sodium ascorbate, and the proteins were then biotinylated in a one-third volume of labeling buffer containing 16 mM PEO-iodoacetyl biotin (Pierce) in HEN buffer at 37 °C for 2 h in the dark. Biotinylated proteins (2 μg) were separated by 12.5% SDS-PAGE and were transferred to a PVDF membrane. The membrane was subjected to Western blotting as described above using mouse anti-biotin monoclonal antibody conjugated with peroxidase at a 1:1000 dilution or goat anti-actin polyclonal antibody (Santa Cruz Biotechnology) at 1:1000 followed by donkey anti-goat polyclonal antibody (Santa Cruz Biotechnology) at 1:5000.

Results

Synthesis and Characterization of Water-Soluble DNICs. The water-soluble RRE complex **DNIC-1**, characterized by IR, UV–vis, and X-ray diffraction analyses, can be synthesized directly by reacting $Fe(CO)_2(NO)_2$ (1 mmol) and 3-mercaptopropionic acid (1 mmol) at 0 °C in THF. The IR spectrum of **DNIC-1** in THF shows three distinct bands in the nitrosyl stretching region ν_{NO} 1751 (s), 1772 (s), 1811 (vw) cm^{-1} , consistent with the formation of RREs. The water solubility of **DNIC-1** is ascribed to the hydrophilic functional group, COOH. To our knowledge, **DNIC-1** is the first water-soluble neutral RRE characterized by X-ray diffraction. As shown in Figure 1, analysis of the bond angles of **DNIC-1** reveals that Fe has a tetrahedral coordination, and the lack of paramagnetism is attributed to the antiferromagnetic coupling between two $\{Fe(NO)_2\}^9$ fragments ($Fe\cdots Fe(A)$, 2.710(3) Å). Upon addition of 2 equiv of diphenylphosphinobenzene-3-sulfonic acid sodium salt to the THF solution of $[Fe(\mu-SC_6H_4-o-NHC(O)Ph)(NO)_2]_2$, a pronounced color change from green yellow to brown occurs at ambient temperature. The formation of **DNIC-2** was confirmed by IR, UV–vis, and FAB-MS.

Assessment of Cytotoxicity of DNICs to Endothelial Cells. To assess the potential cytotoxicity of the synthesized water-soluble DNICs in endothelial cells, EA.hy926 cells were exposed to various concentrations of **DNIC-1** and **DNIC-2** (0.4 μM to

3 mM) in the presence or absence of L-cysteine, which has been known to facilitate the cellular uptake of NO donors such as S-nitrosoglutathione and SNAP.^{53–56} In addition, the cytotoxicity of SNAP, a commonly used NO donor in biological research, was also measured and compared to the results for the two DNIC compounds. As shown in Figure 2A, SNAP-induced cell death occurred in a concentration-dependent manner, with ~50% cell survival at 3 mM. L-Cysteine neither induced cytotoxicity nor altered the cytotoxicity at higher concentrations of SNAP. Similarly, both **DNIC-1** (Figure 2B) and **DNIC-2** (Figure 2C) induced cell death only at high concentrations (> 1 mM). The results indicate that the three NO donors have low cytotoxicity at submillimolar concentrations.

NO-Production Stoichiometry of SNAP, DNIC-1, and DNIC-2. To examine the extent of NO released by **DNIC-1** and **DNIC-2**, the NO production yields were quantified by the Griess assay. The assay measures the total nitrite (NO_2^-) or nitrate (NO_3^-) produced from NO released in an aqueous solution. In the absence of cells, as shown in Figure 3, SNAP, **DNIC-1**, and **DNIC-2** released significant amounts of NO to the medium. SNAP exhibited a rapid, L-cysteine-facilitating NO release that reached a plateau after 0.5 h (Figure 3A). In the presence of L-cysteine, maximal nitrite concentration (~300 μM) revealed a 1:1 stoichiometry of NO release from SNAP. Compared with SNAP, both **DNIC-1** (Figure 3B) and **DNIC-2** (Figure 3C) released significantly more NO with a much slower NO-release rate, producing a maximum of 1200 μM NO at 6 h and 600 μM NO at 24 h, respectively. Interestingly, the presence of L-cysteine enhanced the NO release from **DNIC-1** but had no effect on **DNIC-2**. At 24 h, **DNIC-1** with L-cysteine and **DNIC-2** alone released 4 and 2 equiv of NO per DNIC molecule. Considering the correlation between the molar concentrations and the stoichiometry of NO and Fe (2 NO per atom of Fe), our data indicated complete NO release in the tetranitrosyl-containing **DNIC-1** (in the presence of L-cysteine) and the dinitrosyl-containing **DNIC-2** at 24 h.

We further investigated the variation of measured NO release by NO donors between the cell-containing medium and medium only; i.e. decreased amounts of NO in the presence of cells presumably due to cellular uptake. As shown in Figure 4, the amounts of NO released from 300 μM **DNIC-1** (D1-300) in cell-incubated medium decreased by 80, 180, and 120 μM at 0.5, 2, and 6 h, respectively. In the presence of L-cysteine, the decrease of NO concentration from **DNIC-1** was more profound after 6 and 24 h, having 300 and 240 μM less NO than the medium only. These observations strongly suggest the cellular uptake of **DNIC-1**, and L-cysteine can enhance the uptake. Similarly, the presence of cells resulted in decreased amounts of measurable NO released by **DNIC-2** in the medium, although there was no clear trend with regard to the concentration of **DNIC-2** or the presence of L-cysteine. Taken together, these results demonstrated the cellular uptake of NO in the presence of cells. The possible uptake mechanism was further probed in detail by EPR measurement *vide infra*.

Up-Regulation of HSP70 Expression by DNICs. Malyshey et al. reported that injection of LMW-DNICs into rats resulted in the accumulation of HSP70 in the heart and blood.¹⁹ HSP70 expression was also induced by LMW-DNICs in cultured cells.¹⁹ Because the NO-release data obtained in this study suggest the possibility of cellular uptake of DNICs, we evaluated the efficiency of synthetic DNICs to induce HSP70 accumulation *in vivo*. HSP70 did not accumulate in a low concentration of SNAP stimulation regardless of L-cysteine (Figure 5A and 5B).

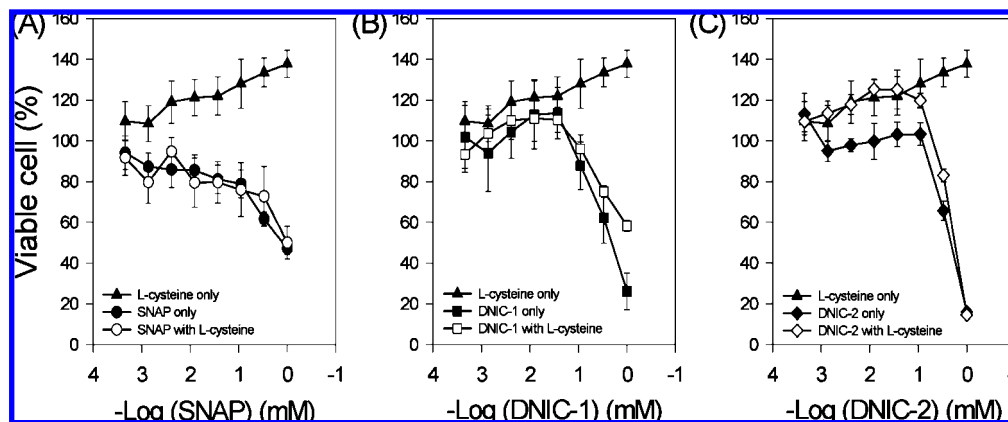


Figure 2. Cytotoxicity of NO donors analyzed by the MTT assay. EA.hy926 endothelial cells were treated by various concentrations (0.4 μM to 3 mM) of NO donor alone or in combination with equal molar L-cysteine and were incubated for 24 h. Cells treated with L-cysteine only served as a control. Cell viability was determined by the MTT assay. The IC_{50} for (A) SNAP, (B) DNIC-1, and (C) DNIC-2 were >1 mM.

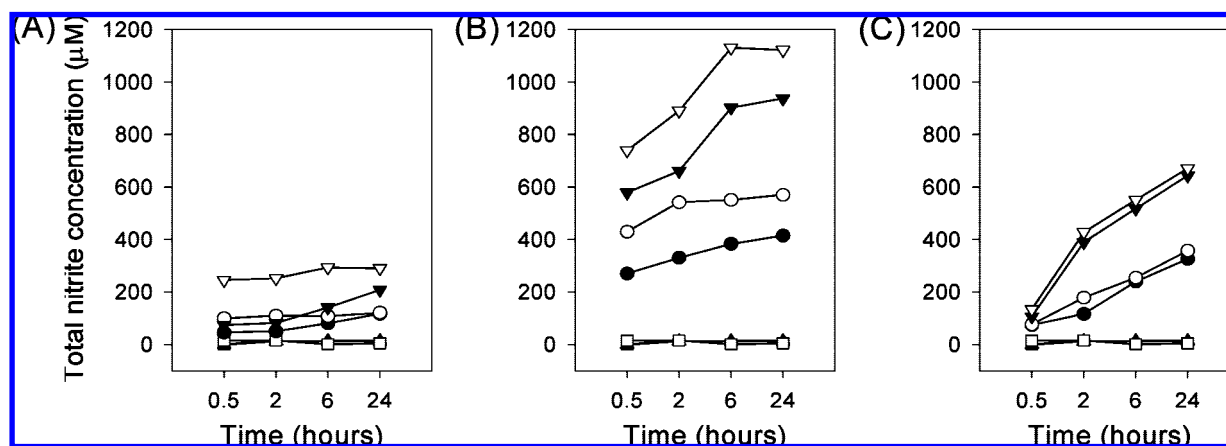


Figure 3. NO release ability of NO donors into cell culture medium. Three NO donors were analyzed: (A) SNAP, (B) DNIC-1, and (C) DNIC-2. NO donor alone, 100 μM (\bullet) or 300 μM (\blacktriangledown), or in combination with 100 μM (\circ) or 300 μM (∇) L-cysteine were added into the medium. Aliquots of treated medium were removed at the indicated times, and the total nitrite concentration was determined by the total nitrite assay kit. Three control experiments, including medium only (\blacktriangle), 100 μM L-cysteine (\blacksquare), and 300 μM L-cysteine (\square) were included for comparison. Note the errors were too small to be drawn on the plot.

In contrast, both 300 μM DNIC-1 and DNIC-2 alone efficiently induced higher HSP70 expression in EA.hy926 cells (Figure 5A). DNIC-1 (300 μM) yielded significant induction of HSP70 in a dose-dependent manner. Weaker HSP70 signals were also observed in a dose-dependent manner in the presence of L-cysteine (Figure 5B). HSP70 was substantially expressed in the presence of 300 μM DNIC-2 alone (Figure 5A), whereas HSP70 overexpression was not affected by addition of L-cysteine (Figure 5B). Our data suggested that DNIC-1 and DNIC-2 are able to physiologically regulate NO-induced activation of HSP70.

Induction of Protein S-Nitrosylation by DNIC-1. *In vivo* S-nitrosylation, which incorporates an NO group in cysteine thiols, has been recognized as a physiologically relevant NO-based protein modification.⁸⁵ To study whether the DNIC-1 acts as an *in vivo* S-nitrosylating agent and to explore its mechanism with regard to understanding possible biological functions of DNIC-1—in particular, the S-nitrosylation of target proteins—we investigated the *in vivo* S-nitrosylation using the biotin-switch method.⁸⁴ In this method, the S-nitrosylated cysteines on the proteins are specifically modified to biotinylated cysteines; other

cysteines in free thiol or disulfide conformations will be blocked by iodoacetamide. Labeled proteins can be then detected by immunoblotting with anti-biotin antibodies. EA.hy926 cells were treated with 300 μM DNIC-1 with L-cysteine. Total cell lysate at different time points (0.5 to 24 h) were harvested and assayed for S-nitrosylation. As shown in Figure 6, DNIC-1 induced a time-dependent increase in *in vivo* protein S-nitrosylation and reached maximal S-nitrosylation at 24 h among the conditions used in this study. In agreement with the aforementioned slow NO release by DNIC-1 as shown in Figures 3 and 4, the similar temporal profile may reveal the specificity of NO-derived regulation of S-nitrosylation. Both results indicate that DNIC-1 can slowly release NO and induce protein S-nitrosylation, confirming that DNIC-1 can act as a slow and long-lived NO donor.

Determination of Structural Conversion and Cellular Uptake of DNIC-1 by EPR Spectroscopy. Because DNIC-1 has demonstrated HSP70 overexpression and *in vivo* protein S-nitrosylation, it was important to address whether DNIC-1 can enter cells and to investigate the possible routes of cellular uptake. EPR spectroscopy, which is sensitive to paramagnetic metal centers, was used to probe the conversion of diamagnetic water-soluble DNIC-1 to paramagnetic intermediates. The paramag-

(85) Hess, D. T.; M, A.; Kim, S.-O.; Marshall, H. E.; Stamler, J. S. *Nat. Rev. Mol. Cell Biol.* 2005, 6, 150–166.

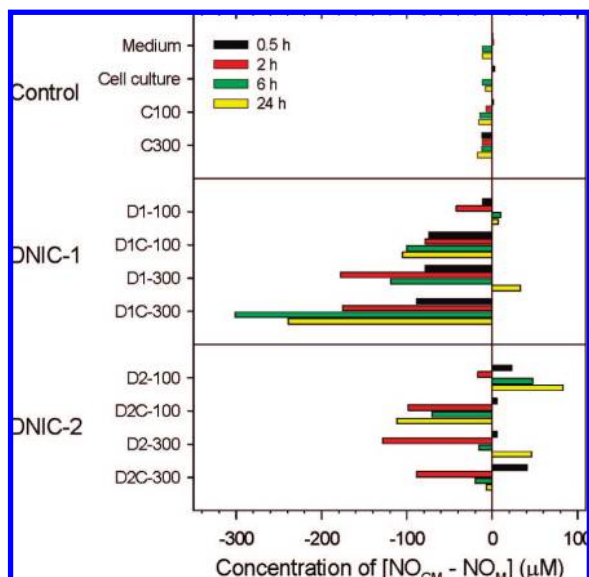


Figure 4. Differential release of NO in medium containing cells and medium only. EA.hy926 cells were treated with 100 μM of **DNIC-1** (D1-100) or **DNIC-2** (D2-100) alone, 100 μM of **DNIC-1** with L-cysteine (D1C-100) or **DNIC-2** with L-cysteine (D2C-100), 300 μM of **DNIC-1** (D1-300) or **DNIC-2** (D2-300) alone, or 300 μM of **DNIC-1** with L-cysteine (D1C-300) or **DNIC-2** with L-cysteine (D2C-300) for the indicated times. Aliquots of the medium were removed at each time point, and the total nitrite concentration was determined by the total nitrite assay kit. The differences of the nitrite amount in the presence (NO_{CM}) or absence (NO_{M}) of cells were calculated and plotted. Negative nitrite concentration indicates cellular uptake of NO.

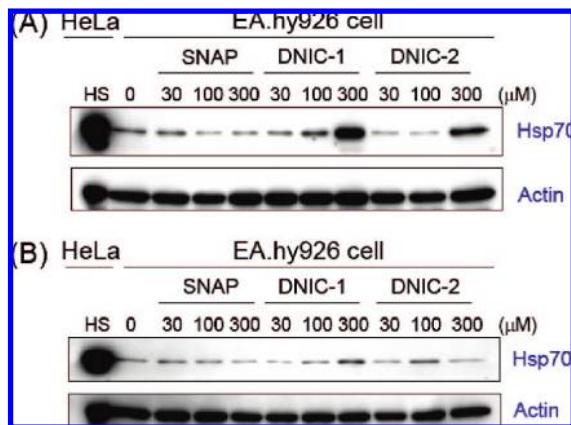


Figure 5. Induction of HSP70 expression by NO donors. EA.hy926 endothelial cells were treated with the indicated concentrations of SNAP, **DNIC-1**, or **DNIC-2** alone (A) or with equal molar L-cysteine (B) for 24 h. Total cell lysate (1 μg) was subjected to Western blotting using mouse anti-HSP70 (Actin served as a loading control). Total cell lysate from heat-shocked (HS) HeLa cells (2 μg) was included as a positive control.

netic characteristics of DNICs are sensitive to the electronic structure and the coordination environment of complexes.^{72,86,87} Although dinuclear $\{\text{Fe}(\text{NO})_2\}_2$ - $\{\text{Fe}(\text{NO})_2\}_2$ **DNIC-1** is EPR silent, $\{\text{Fe}(\text{NO})_2\}_2$ DNIC gives an axial EPR pattern with $g_{\perp} = 2.04$ and $g_{\parallel} = 2.01$ under liquid nitrogen temperature (77 K). To systematically probe the cellular uptake of **DNIC-1**, we first examined the conversion of **DNIC-1** from dinuclear $\{\text{Fe}(\text{NO})_2\}_2$ -

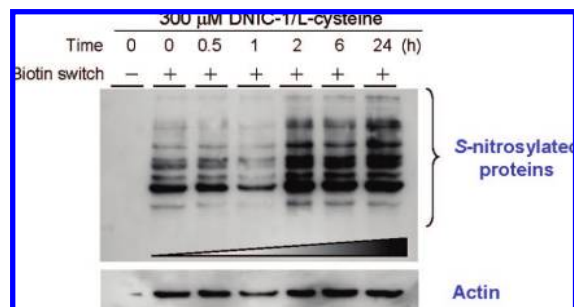


Figure 6. Detection of S-nitrosylated proteins in EA.hy926 cells using the biotin switch method. Cells were treated by 300 μM **DNIC-1** with equal molar of L-cysteine and incubated in the dark for indicated time. S-nitrosylated proteins in the total cell lysate were detected by the biotin switch method. In parallel, total cell lysate without the biotin switch served as a negative control, and Actin served as a loading control. At 0.5 to 24 h, *in vivo* S-nitrosylated signals from the **DNIC-1** treatment can be observed.

$\{\text{Fe}(\text{NO})_2\}_2$ to mononuclear $\{\text{Fe}(\text{NO})_2\}_2$ DNIC in the medium with or without L-cysteine. As shown in Figure 7A (black line), strong EPR signals with $g_{\perp} = 2.04$ and $g_{\parallel} = 2.01$ suggesting the presence of $\{\text{Fe}(\text{NO})_2\}_2$ DNIC were observed when 300 μM **DNIC-1** was incubated in the medium for 15 min. The time-course measurements revealed a 2.5-fold enhancement in EPR signal after 6 h (red line, Figure 7A). Interestingly, the addition of 1 equiv of L-cysteine with **DNIC-1** in the medium resulted in rapid formation of EPR signals in 15 min and decay to one-half of the maximum intensity after 6 h (compare green and blue lines, Figure 7A). These results suggest that dinuclear **DNIC-1** was converted to mononuclear $\{\text{Fe}(\text{NO})_2\}_2$ DNIC in the medium and that L-cysteine accelerated this conversion. The latter observation is also consistent with enhanced NO release from **DNIC-1** in the presence of L-cysteine as observed in the total nitrite assay (Figure 3). Therefore, L-cysteine may accelerate **DNIC-1** conversion as well as promote the decomposition of the EPR active $\{\text{Fe}(\text{NO})_2\}_2$ DNIC to Cys-NO.

We next studied the conversion of **DNIC-1** in the presence of EA.hy926 cells. EPR signals of $\{\text{Fe}(\text{NO})_2\}_2$ DNIC from **DNIC-1** were detected in the cell cultured medium after 15 min, and L-cysteine enhanced the signals (black and green lines, Figure 7B). The signals were also comparable to those in the control medium, or medium without cells (Figure 7A). However, the $\{\text{Fe}(\text{NO})_2\}_2$ DNIC signals decayed much faster in the cell cultured medium (compare red lines in Figure 7A and 7B), and no residual signal was observed in the presence of L-cysteine after 6 h (blue line, Figure 7B). Interestingly, EPR signals of $\{\text{Fe}(\text{NO})_2\}_2$ DNIC were observed in **DNIC-1**-treated EA.hy926 cells after 15 min regardless of the presence of L-cysteine (black and green lines, Figure 7C). The intracellular $\{\text{Fe}(\text{NO})_2\}_2$ EPR signal may have resulted from direct transportation of intact **DNIC-1** followed by structural conversion to $\{\text{Fe}(\text{NO})_2\}_2$ DNIC, conversion of **DNIC-1** to $\{\text{Fe}(\text{NO})_2\}_2$ DNIC in the medium followed by transportation of $\{\text{Fe}(\text{NO})_2\}_2$ DNIC into the cells, or the reassembled DNIC inside the cells using NO (originated from **DNIC-1**) together with intracellular RSH and Fe^{2+} . To further understand the origin of the intracellular EPR signals, we performed the same experiment using SNAP. No EPR signal was observed in SNAP/L-cysteine treated cells (red line, Figure 7D). Weak but conclusive $\{\text{Fe}(\text{NO})_2\}_2$ DNIC signals were detected only in the cells preincubated with excess FeSO_4 , acting as an iron source, for 12 h prior to **DNIC-1** treatment (blue line, Figure 7D). These data showed that the intracellular iron concentration in EA.hy926 cells is not sufficient to form $\{\text{Fe}(\text{NO})_2\}_2$ DNIC when NO is present.

(86) Vanin, A. F.; Serezhnikov, V. A.; Mikoyan, V. D.; Genkin, M. V. *Nitric Oxide* **1998**, *2*, 224–234.

(87) Boese, M.; Mordvintsev, P. I.; Vanin, A. F.; Busse, R.; Mulsch, A. *J. Biol. Chem.* **1995**, *270*, 29244–29249.

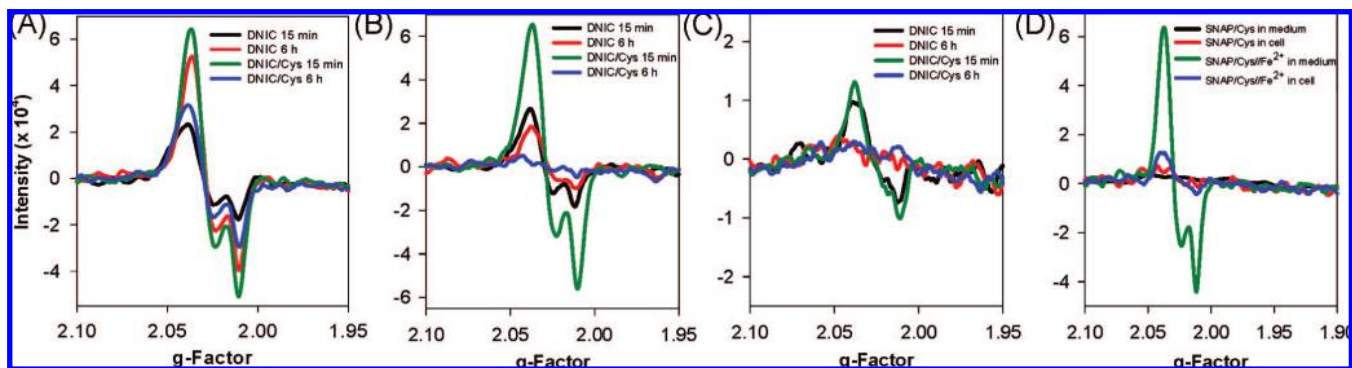


Figure 7. EPR spectra obtained from **DNIC-1**-treated cell culture medium and cultured cells. 300 μM **DNIC-1** was incubated with or without an equal molar ratio of L-cysteine (A) in control medium, (B) in cell cultured medium, and (C) in cells for 15 min or 6 h. Control experiment shown in (D) was performed using 1.2 mM SNAP/L-cysteine mixture incubated alone or with 0.25 mM Fe^{2+} in control medium and cells for 15 min.

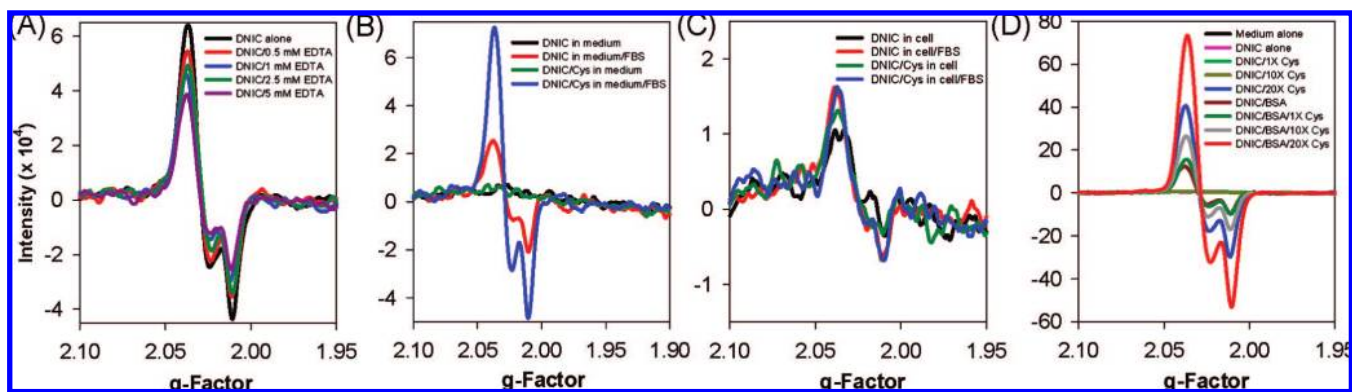


Figure 8. EPR spectra showed that **DNIC-1** conversion was assisted with serum/BSA or surplus L-cysteine. (A) EDTA (0 to 5 mM) was incubated with 300 μM **DNIC-1** in control medium for 15 min. (B) 300 μM **DNIC-1** alone or with L-cysteine was incubated in serum-free medium or complete medium for 15 min. (C) Cell signal from cells incubated in serum-free medium or in complete medium treated with 300 μM **DNIC-1** alone or with L-cysteine for 15 min. (D) EPR spectra from serum-free medium treated with 300 μM **DNIC-1** with or without 1% BSA and 0 to 20 equiv of L-cysteine for 15 min, respectively. The signals of serum-free medium containing 300 μM **DNIC-1** alone and with 1 or 10 mol equiv of L-cysteine were in the background level.

Previous studies on the electronic structure of **DNIC-1** type complexes confirmed that the compound is EPR silent and is stable in organic solvent.⁶⁴ In our analysis, however, EPR signals were detected in aqueous environments, such as the cell culture medium. Our observations prompted us to study the roles of the cell culture medium in cellular uptake as well as **DNIC-1** conversion, which is important to understand the identity of $\{\text{Fe}(\text{NO})_2\}^9$ DNIC. Interestingly, an EPR signal of $\{\text{Fe}(\text{NO})_2\}^9$ DNIC was observed in the control medium with SNAP/L-cysteine and Fe^{2+} , whereas no signal was detected in the SNAP/L-cysteine control medium without Fe^{2+} (green and black line, Figure 7D). The result indicated that, in the presence of Fe^{2+} and L-cysteine, reassembly of $\{\text{Fe}(\text{NO})_2\}^9$ DNIC can take place *in situ* in the solution. To explicitly exclude potential **DNIC-1** decomposition to RSH, NO, and Fe^{2+} as contributing to the reassembly of $\{\text{Fe}(\text{NO})_2\}^9$ DNIC in solution, we added EDTA to remove any Fe^{2+} from potential **DNIC-1** decomposition. As shown in Figure 8A, EDTA did not fully deplete the $\{\text{Fe}(\text{NO})_2\}^9$ DNIC EPR signal when 0.3 mM **DNIC-1**, which contains 0.6 mM of equivalent Fe^{2+} , incubated with an equal (0.5 mM) to 8-fold (5 mM) molar equivalent of EDTA. These results indicated the EPR signal from **DNIC-1** in solution was not reassembled from decomposition of **DNIC-1** but directly converted from **DNIC-1**. When the composition of the culture medium was further examined, it contains nutrients, such as amino acids, sugars, and animal sera, i.e., fetal bovine serum (FBS), as the source of growth hormones. To dissect the role

of the cell culture medium in **DNIC-1** conversion, the paramagnetic DNIC signals were compared in a serum-free or complete medium. EPR signals of $\{\text{Fe}(\text{NO})_2\}^9$ DNIC were detected in the complete medium but not in a serum-free medium (red and black lines, Figure 8B). The presence of L-cysteine enhanced the EPR signals in the complete medium (medium/FBS), but no signal was observed in the serum-free medium (blue and green lines, Figure 8B). These data suggest that fetal bovine serum is the key ingredient in the medium for **DNIC-1** conversion. Collectively, these data demonstrated that **DNIC-1** can stably exist in aqueous solution. In addition, intracellular EPR signals from **DNIC-1**-treated cells were observed in both complete and serum-free mediums (Figure 8C), suggesting that the transport of **DNIC-1** into cells was independent of the components of the cell culture medium and, importantly, demonstrating that **DNIC-1** permeated directly into cells.

We next ask which component in the FBS attributes to **DNIC-1** conversion. The FBS contains $\sim 70\%$ bovine serum albumin (BSA). Previous literature has reported that BSA reacts with LMW-DNICs to form EPR-active protein-bound DNICs.⁸⁷ To study whether BSA acts in a similar way in our system, **DNIC-1** was incubated with 1% BSA in a serum-free solution and analyzed by EPR spectroscopy. **DNIC-1** rapidly converted to the EPR-active form when incubated with BSA (brown line, Figure 8D), indicating the formation of a BSA-bound DNIC. Increasing the amount of L-cysteine enhanced the formation of

the BSA-bound DNIC (green, purple, and red lines, Figure 8D). To our surprise, a strong L-cysteine-DNIC signal was observed in **DNIC-1** with at least a 20-fold molar surplus of L-cysteine in the serum-free medium (blue line, Figure 8D). These data suggest that the formation of protein-bound $\{\text{Fe}(\text{NO})_2\}^9$ BSA-DNICs predominates in the presence of serum, whereas, in the absence of serum, conversion of **DNIC-1** to low-molecular-weight L-cysteine-DNIC proceeds only with high concentrations of L-cysteine.

Discussion

In this study, the biological activities of two novel water-soluble synthetic DNIC complexes, **DNIC-1** (RRE) and **DNIC-2** ($\{\text{Fe}(\text{NO})_2\}^{10}$ DNIC), were investigated. Compared with SNAP, **DNIC-1** and **DNIC-2** produced slower yet 4-fold and 2-fold higher levels of NO under physiological conditions, respectively. The similar NO-release stoichiometry was also demonstrated in another water-soluble RRE, $\text{Na}_2[\text{Fe}_2(\text{SCH}_2\text{CH}_2\text{SO}_3)_2(\text{NO})_4]$, undergoing photodecomposition under aerated solutions (3.8 mol of NO per mole of RRE).⁸⁸ Although differential NO-releasing property of the three investigated NO donor compounds were observed, they exhibited similar cytotoxicities. Previous evidence has shown that, in the presence of equal concentrations of NO-donor compounds, long half-life NO-donor species protect cells, whereas the short half-life NO-donor species promote apoptosis.⁸⁹ This indicates that the rate of NO production is an important factor for NO-mediated cell death. Our cytotoxicity results also support this argument. At low concentrations of **DNIC-1** or **DNIC-2** ($<300 \mu\text{M}$), no significant cytotoxicity was observed presumably due to the slow NO release from these NO-donor compounds. Higher concentrations of **DNIC-1** or **DNIC-2** (e.g., $>1 \text{ mM}$), however, resulted in greater NO production and significantly increased programmed cell death. In this study, **DNIC-1** proved to be a better NO donor species compared with $\{\text{Fe}(\text{NO})_2\}^{10}$ **DNIC-2**,^{64,66} because 4-fold increases of NO from **DNIC-1** and 2-fold increases of NO from **DNIC-2** were released as compared with SNAP.

It has been reported that NO and NO donors induce HSP70 expression and exert a cardioprotective effect.^{19,90} The prominent ability of **DNIC-2**, and especially **DNIC-1**, to induce HSP70 overexpression also suggests their potential to have a cardioprotective effect in vascular endothelial cells. Regardless of the presence of L-cysteine, our data indicate that **DNIC-1** induces HSP70 accumulation. Together with the decreased amount of NO in the presence of cells, we hypothesized that **DNIC-1** relies on a mechanism involving either passive diffusion or transporters to permeate cell membranes and release NO inside cells. The ability of **DNIC-1** to induce protein S-nitrosylation *in vivo* further supports this argument. The prolonged *in vivo* protein S-nitrosylation signals by **DNIC-1** after 24 h of incubation again suggest that **DNIC-1** behaves as a long-stability NO donor.

To our knowledge, the present EPR spectroscopic data reveal the first detailed picture for the interconversion and cellular permeation pathways of **DNIC-1**. The EPR results reconcile that dinuclear **DNIC-1** is converted into either a protein-bound form or a low-molecular-weight thiolate coordinated to

$\{\text{Fe}(\text{NO})_2\}^9$ DNIC. In the absence of L-cysteine, our data confirmed that **DNIC-1** converts to a protein-bound DNIC with BSA and shows slow NO release. Excess L-cysteine accelerates not only the conversion of **DNIC-1** into $\{\text{Fe}(\text{NO})_2\}^9$ DNIC but also NO release from $\{\text{Fe}(\text{NO})_2\}^9$ DNIC. The role of L-cysteine in accelerating NO release from **DNIC-1** was also confirmed by the total nitrite assay. Taken together, we concluded that excess L-cysteine induced rapid LMW-DNIC formation from **DNIC-1** and promoted NO release, whereas the much slower NO release of **DNIC-1** was attributed to the more stable protein-bound DNIC, presumably through the transfer of the $\text{Fe}(\text{NO})_2$ group to BSA in the cell culture medium.⁵⁹

The EPR signal of **DNIC-1** observed in the cells is intriguing. Because BSA-DNICs have been confirmed to be the major form in the medium in either the presence or absence of L-cysteine, our data suggest that, in the complete medium, the EPR signal observed inside cells originates either from the transport of intact **DNIC-1** or from the transport of BSA-DNIC into cells. With surplus L-cysteine in the serum-free medium, the EPR signal in cells likely originates from imported intact **DNIC-1** or a low-molecular-weight L-cysteine-bound DNIC. The detection of intracellular $\{\text{Fe}(\text{NO})_2\}^9$ DNIC under serum-free and L-cysteine-free conditions confirms the direct transport of intact **DNIC-1** into the cells as well as its conversion to $\{\text{Fe}(\text{NO})_2\}^9$ DNIC. It is unlikely that EPR signals originated from reassembly of a DNIC from NO, thiols, and intracellular Fe^{2+} inside the cells, because the intracellular iron concentration in EA.hy926 cells is too low to reassemble EPR detectable a DNIC from imported NO. Intracellular EPR signals from FeSO_4 pretreated cells, for which the intracellular Fe^{2+} concentration was elevated, after the addition of SNAP and L-cysteines further supported our argument. Currently, because of the complicated cellular environment and relatively low concentration of DNIC, the identity of DNICs inside cells remains to be determined. Noticeably, EPR signals in the cells remain constant regardless of the presence of L-cysteine, indicating a basal level of $\{\text{Fe}(\text{NO})_2\}^9$ DNIC inside cells.

Figure 9 presents a hypothetical model for **DNIC-1** conversion and three major routes of **DNIC-1** uptake by cells summarized from the results described above. *Route 1*: Intact **DNIC-1** can be transported into cells in the absence of L-cysteine and serum. *Route 2*: In the presence of serum, **DNIC-1** is converted to BSA-bound $\{\text{Fe}(\text{NO})_2\}^9$ DNIC and subsequently transported into cells. *Route 3*: In the absence of serum, alternatively, **DNIC-1** can be converted to $[\text{DNIC}-(\text{Cys})_2]$ in the presence of excess L-cysteine and then be transported into cells. The possibility of extracellular interconversion between different DNIC forms remains to be investigated. Conversion of **DNIC-1** into a form that is undetectable by EPR spectroscopy and cell permeation as NO or Cys-NO (*route 4*) also cannot be ruled out. After cellular entry through one of these proposed routes, the different forms of DNIC presumably can induce protein nitrosylation and produce other cellular responses.

Concluding Remarks

We presented herein the biological activity and EPR study of the well-characterized low-molecular weight DNICs using EA.hy926 as the cell model. In summary, our data demonstrated the following:

1. A well-characterized synthetic water-soluble RRE **DNIC-1**, for the first time, behaved as a long-lived yet slow NO-releasing species with a defined stoichiometry (4 NO per molecule) under physiological conditions. Similar to **DNIC-1**,

(88) Conrado, C. L.; Bourassa, J. L.; Egler, C.; Weckler, S.; Ford, P. C. *Inorg. Chem.* **2003**, *42*, 2288–2293.

(89) Rosenberg, P. A.; Li, Y.; Ali, S.; Altiock, N.; Back, S. A.; Volpe, J. J. *J. Neurochem.* **1999**, *73*, 476–484.

(90) Xu, Q.; Hu, Y.; Kleindienst, R.; Wick, G. *J. Clin. Invest.* **1997**, *100*, 1089–1097.

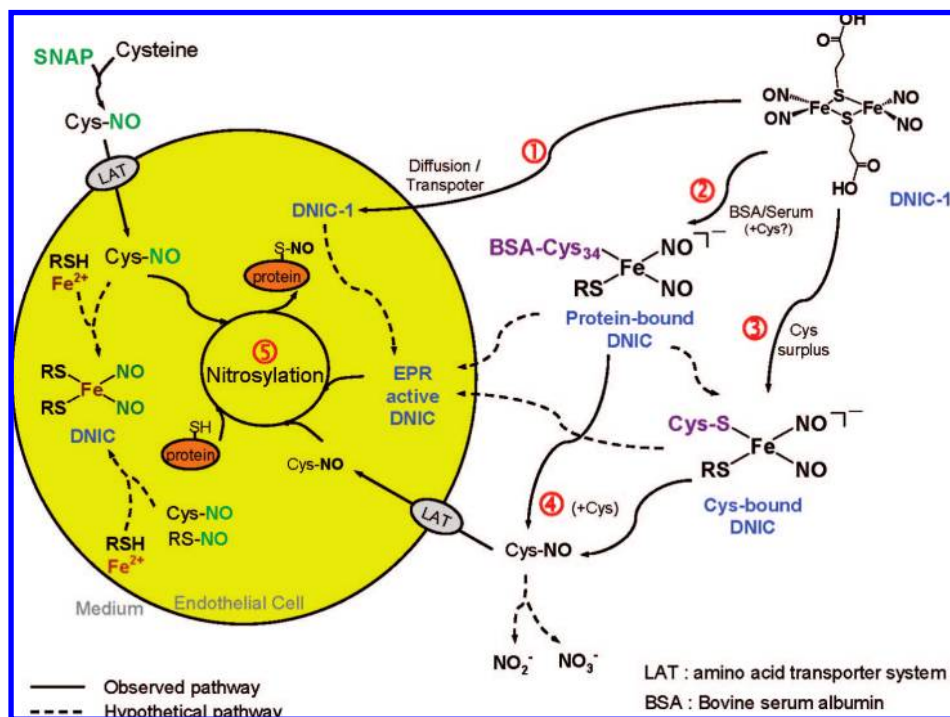


Figure 9. Model for conversion and cellular transportation of **DNIC-1**. See text for detailed description.

the $\{\text{Fe}(\text{NO})_2\}^{10}$ **DNIC-2** also acted as a slow NO-releasing compound under physiological conditions with a releasing stoichiometry of 2 NO per molecule.

2. **DNIC-1** and **DNIC-2** showed low cytotoxicity ($<300 \mu\text{M}$) and induced HSP70 overexpression, as well as protein S-nitrosylation *in vivo*.

3. The first delineation of the cellular uptake mechanism of RRE was uncovered by EPR spectroscopic evidence. **DNIC-1** can either directly permeate into cells or be transported into the cells by protein-bound or LMW-DNIC species.

To further dissect the physiological role of **DNIC-1** and its target molecules, we are currently conducting a large-scale identification of proteins that are S-nitrosylated upon **DNIC-1** stimulation. Furthermore, quantitative proteomics will be performed in the near future to shed light on the signaling cascade and mechanism.

Acknowledgment. The work was supported by the National Council of Science (NSC-94-2627-M-007-001, NSC 95-2627-M-007-001) and Academia Sinica, Taiwan. We thank Dr. Tsu-Ching Meng at the Institute of Biological Chemistry, Academia Sinica, for providing the EA.hy926 cell line and critical discussion and Ms. Ping-Yu Lin at the Institute of Chemistry for the HR-FAB MS analysis.

Supporting Information Available: IR and UV-vis spectra of **DNIC-1** and **DNIC-2** in THF solution; mass spectra of **DNIC-1** by FAB-MS analysis and **DNIC-2** by high resolution FAB-MS analysis. This material is available free of charge via the Internet at <http://pubs.acs.org>.

JA711494M